JOTCS A
Journal of the Turkish Chemical Society
Section: A
Chemistry
TURKISH CHEMICAL SOCIETY

Curing Kinetic Analysis and Isothermal Prediction of DBTL Catalyzed Polyurethane Reaction by Differential Scanning Calorimetry

Seçil Sevim Ünlütürk* and **Necati Güdümcüoğlu**

Kansai Altan Paint Industry and Trade Inc.

Abstract: Kinetic analysis is generally carried out to clarify the reaction mechanism with kinetic parameters and to predict the kinetic properties of materials under different reaction parameters. The kinetics of the polyurethane polymerization reaction between acrylic polyol and isocyanate was investigated by Differential Scanning Calorimetry (DSC) in terms of catalyst amounts and sampling times. Single and multiple heating analyses were used to obtain DSC curves for each sample. The simple kinetic model and Multilinear Regression Fit (MRF) were used to calculate the kinetic parameters and simulate the isotherm prediction curves. The kinetic calculations showed that the glass transition temperatures (up to 44 °C) and activation energy (Ea) values increased with the degree of conversion for all cases. The reduction in the rate constant for partially cured samples was greater than the initial sampling time of the same sample. This observation indicates that the diffusion controlled reaction dominates and Ea increases due to the highly cross-linked and dense medium in partially cured samples. Isothermal prediction curves provide an understanding of different curing conditions at different reaction temperatures and times. Prediction curves show slower conversion even for final samples, confirming that final samples may remain uncured. Applying the results of this study, especially for real-world applications, where fully cured samples are required, additional annealing procedures can be easily established.

Keywords: Polyurethane, Curing Kinetic, Differential Scanning Calorimetry

Submitted: March 22, 2024. Accepted: June 12, 2024.

Cite this: Ünlütürk SS, Güdümcüoğlu N. Curing Kinetic Analysis and Isothermal Prediction of DBTL Catalyzed Polyurethane Reaction by Differential Scanning Calorimetry. JOTCSA. 2024;11(3):1211–24.

DOI: https://doi.org/10.18596/jotcsa.1441231.

*Corresponding author. E-mail: sclsvm@gmail.com.

1. INTRODUCTION

Polyurethanes are widely used polymeric materials in foams, coatings, adhesives, insulators, etc. They are very popular especially in automobile coatings due to their advantages in terms of weathering, appearance, chemical and mechanical resistance, etc.(1) All these advantages are provided by controlling the reaction kinetics of the polymeric matrix. In other words, understanding the rate of the chemical reaction is critical in terms of deciding the desired outcomes of the chemical reaction.

Kinetic analysis is very popular in terms of both understanding the reaction mechanism by describing the kinetic process and the kinetic prediction of the reaction in different reaction parameters. Generally, the kinetic process can be defined with the kinetic triplet which are the activation energy (Ea), the pre-exponential factor (A), and the reaction model (f(a)). The activation energy is the energy barrier for the reaction. It is valuable to evaluate the reaction parameters like reaction temperature, time, etc., and accordingly the desired product yield. While the pre-exponential factor can be described as the vibrational frequency of the activated complex, the reaction model is directly relevant to the reaction mechanism (2). The reaction model can be autocatalyzing or nth order depending on the reaction mechanism. An autocatalytic process due to the formation of hydroxyl groups in an epoxy system was studied by Yi et al. to understand the solvent effect of the system(3). On the other hand nth order curing reaction model is accepted as the simplest way to describe the curing kinetic reactions of thermosetting plastics(4) like polyurethanes.

Several techniques can be used to evaluate the reaction kinetics. Viscosity measurements were preferred to estimate the reaction kinetics by Manu et al. but they work only below the gel point of the materials(5) which limits to study of other materials.

Techniques like gel permeation chromatography (GPC) and nuclear magnetic resonance (NMR) spectroscopy are also tools to study the reaction kinetics. However, the insolubility of materials in organic solvents restricts the usage of these techniques(6). Epoxy amine reactants can be considered as an example of this case that the recently cured products are insoluble in the organic solvent that is used in these methods. Additionally, these kinds of techniques require critical expertise it is difficult to analyze the spectra. The presence of numerous methyl and methylene groups makes the NMR spectrum very complex. Similarly, GPC, may not be very realistic or indicative due to the highly branched polymer structure(7). Apart from these thermal analysis like thermal gravimetric analysis (TGA) or differential thermal analysis (DTA) and mostly differential scanning calorimetry (DSC), can be used for the determination of the curing reactions. (8, 9)

In this study, the reaction between an isocyanate and acrylic polyol curing reaction was investigated by the non-isothermal method of DSC. The isothermal method was not preferred because there is an inconsistency caused by the fact that a significant part of the cure reaction occurs before the set isothermal temperature is reached. The non-isothermal method includes single and multiple heating rate procedures. In this study, mainly a single heating rate was used because of its advantage of being fast and valuable in comparative studies such as evaluating the relative efficiencies of various catalysts. (7) Dibutyltin dilaurate catalyst which is one of the popular organo-tin catalysts in the production of polyurethanes because of its strong catalytic activity towards diisocyanates and polyols(10) was used. Different amounts of DBTL were added to understand its effect on the kinetic reaction of PUR. Since it is known that PUR reactions have second-order reaction kinetic(11), nth-order reaction kinetics were applied for the samples with 0, 0.01, 0.1, and 0.5 phr (per hundred resin) catalyst amounts in different curing periods. Results were investigated by the calculations according to the simple kinetic model and Multilinear Regression fit (MRF). The isoconventional predictions were evaluated in terms of % conversion concerning reaction time and temperature for different isothermal temperatures and reaction times, respectively. The curing results were also proved by Dynamic Mechanical Analysis, DMA too.

2. EXPERIMENTAL SECTION

2.1. Materials and Preparation

The polyurethane polymer matrix in which commercially available acrylic polyol and modified isocyanate were reacted was used in this study. Butyl acetate was chosen as the solvent. Dibutyltin dilaurate (DBTL) which is a highly reactive solvent-free tin catalyst was added in different amounts to study the effect of catalyst amount on the curing kinetics of the PUR system. Four different samples, C1, C2, C3, and C4 were studied as the catalyst amounts were 0, 0.01, 0.1, and 0.5 phr, respectively. The NCO:OH molar ratio was arranged as 1:1 for all samples. The representative structure of the PUR reaction between polyol and isocyanate is given in Figure 1.

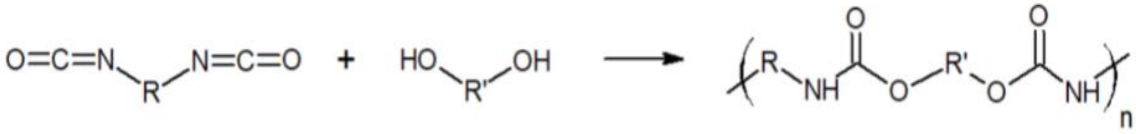

Figure 1. The representative structure of PUR reaction between polyol and isocyanate

Reactants were mixed with Cowles type mixer for 15 minutes at 350 rpm to have a homogenous mixture. The samples were applied to tinplate by 50 µm applicators to have uniform films. Different periods were selected for DSC analysis. For each sample, t_0 (after flash-off time at room temperature - 15 minutes after application), $t_{30min\text{-}80C}$ (30 minutes at 80°C annealing after 15 minutes flash-off time), and t_{final} (1 week after 30 minutes at 80°C annealing process and 15 minutes flash-off time) sampling periods were chosen and analyzed in DSC separately. Flash-off time is the necessary waiting time to coat/recoat on a freshly coated surface. DMA analysis for each sample was also applied for Day 1 and Day 7 to understand and compare the effect of catalyst amount on the curing mechanism. Since free films are required for DMA analysis, the same samples were applied to Polypropylene (PP) substrates. Free films of the samples cannot be obtained before Day 1 because of not curing sufficiently.

2.2. Differential Scanning Calorimetry (DSC) Kinetic Measurements

The glass transition temperatures (Tg) and curing kinetics of PUR systems with and without dibutyltin dilaurate catalyst were investigated by DSC 8000, Perkin Elmer. Non-isothermal, also called as isoconventional method was used under different heating rates between -20°C and 200°C temperature ranges. The non-isothermal method was preferred instead of the isothermal method because of obtained relatively more reliable information according to the Kinetics Committee of the International Confederation for Thermal Analysis and Calorimetry (ICTAC) recommendations (12). As mentioned before, inconsistent results may be obtained since a significant part of the material cured during the heat rise to the set isothermal temperature

For the multiple heating methods, the heating rates of 2.5, 5, 10, 20, and 50 K/min were considered. A nitrogen atmosphere was arranged as a constant flow of 50 mL/min. The thermal data obtained from heat

flow as a function of temperature was used to determine both Tg and curing enthalpy of the system. The calibration of DSC was checked by melting temperature and the melting enthalpy of the Indium standard. The curing curves were subtracted from the background curves which were obtained by the same procedure, the same pan (Image S1) but without the sample in it. Isothermal predictive curves are also obtained in terms of % conversion variation concerning time and reaction temperature at different isothermal temperatures and reaction times, respectively.

2.2.1 Theoretical Approach

Theoretically, the reaction rate "n", depends on two variables; temperature "T", and the conversion degree "a". If the reactants and/or products are in the gas form, pressure is also needed as a required term(12). However, there is no reactant or product in gas form in the PUR reaction mechanism. Also, there is an external gas flow in thermal analysis as 50 mL/K. Consequently, the pressure is forced to be constant and neglected in the rate equation that is considered.

$$v = \frac{d\alpha}{dt} = k(T)f(\alpha) \quad (1)$$

In the equation above, $k(T)$ is the specific rate constant at temperature T and $f(\alpha)$ is the reaction model. The equation is used to describe the rate of a single-step process. If the process is accompanied by the releasing/absorption of heat as measured in DSC, the conversion degree "a" is evaluated by a ratio of curing enthalpy at time t (ΔH_t) to the total curing enthalpy (ΔH_T). Total curing enthalpy can be found experimentally by calculating the area under the curing peak of the uncured sample. Representative image was shown in Figure S1.

$$\alpha = \frac{\Delta H_t}{\Delta H_T} \quad (2)$$

In this case, the conversion degree changes between 0 and 1 as the progress of the process. It can also be named as % Conversion with a variation between 0 and 100. The important point that should be in mind is that the physical properties measured by thermal analysis like DSC can not be related to a specific reaction. As mentioned before, it only gives information about the overall transformation of the reaction. (12)

In the PUR case, the reaction obeys the second-order reaction kinetics. (11, 13, 14) That is the reason nth order reaction model was accepted. The kinetic calculations were done by the scanning kinetics model which assumes the simple kinetic model and uses Multilinear Regression fit (MRF) to curve fit. Whenever a peak is detected on a DSC curve when the sample is subjected to a controlled temperature ramp, it can be assumed that there has been a transformation. This can be represented as the following chemical reaction;

$$A \xrightarrow{k} B + \Delta H \quad (3)$$

Where, A and B are the materials before and after the conversion, respectively. k is the reaction rate as mentioned before and ΔH is the enthalpy (heat) of the chemical reactions or the physical transition. For the kinetic calculations, the rate of the reaction, the change of reactants to products, and related time/temperature were the concerned terms. The combination of the Eq.1 and 2 give the following which shows the n^{th}-order reaction kinetic with respect to time.

$$\frac{d\alpha}{dt} = k(1-\alpha)^n \quad (4)$$

Combining the Arrhenius equation (Eq.5) which is used to define rate constant and Eq.4, the final equation is obtained as Eq.6.

$$k(T) = A\exp(-\frac{E_a}{RT}) \quad (5)$$

$$\frac{d\alpha}{dt} = A\exp(-\frac{E_a}{RT})\,(1-\alpha)^n \quad (6)$$

where A and E_a are the pre-exponential factor and the activation energy, respectively. R is the universal gas constant (15). The activation energy, pre-exponential factor, and the reaction model, which are named as kinetic triplet, should be described to understand the overall kinetic process of the reaction mechanism. While the activation energy can be defined as the barrier to the reaction starts, the pre-exponential factor is the vibrational frequency of the activated complex. The reaction model is directly linked to the reaction mechanism(2). In this equation, there is one independent variable t, two dependent variables α and T, three unknown constants A, Ea, and n, and the universal gas constant, R.

In DSC, temperature varies with time linearly as shown below;

$$T - T(0) = \beta.t \quad (7)$$

$$\beta = \frac{dT}{dt} \quad (8)$$

Where t is the time, β is the scanning rate, and T and T(0) are the current and initial temperatures, respectively. s time, and β is the scanning rate. All the calculations in this study were done by the following equation which represents the theoretical shape of the DSC curve and obtained by the combination of the eq.8 and 6.

$$\beta\frac{d\alpha}{dt} = \mathrm{A}\exp(-\frac{E_a}{RT})\,(1-\alpha)^n \quad (9)$$

The obtained DSC curves were fitted by the equation 9 or 6 in which the only difference is the unit as dt or dT. A, Ea and n values can be calculated by single DSC curve by having ΔH_t as mentioned in Eq.2. Since there are three unknown parameters, multilinear regression is used by reducing the linear form of equation above (Eq.9). A multilinear regression is performed to solve these three unknown variables by using $(\ln\beta\frac{d\alpha}{dt})$, $-\frac{1}{RT}$, and $ln(1-\alpha)$ as variables evaluated from DSC data.

On the other hand, the model-free approach was also discussed. Different approximations exist to solve the temperature integral, but Ozawa and Kissinger's equations are very popular in terms of the relationship between activation energy and heating rate, temperature as given below.

Ozawa equation (16);

$$-\ln(\beta) = 1.0516\left(\frac{E_a}{RT_p}\right) - A \qquad (10)$$

Kissinger equation (17);

$$-\ln\left(\frac{\beta}{T_p^2}\right) = \left(\frac{E_a}{RT_p}\right) - \ln\left(\frac{AR}{E_a}\right) \qquad (11)$$

In the equations above, β is the heating rate. From the first equation, Ozawa, a plot of $-\ln(\beta)$ vs. $\left(\frac{1}{T_p}\right)$ gives a straight line as a slope that the activation energy can be calculated. Similarly, from the second equation, Kissinger, a plot of $-\ln\left(\frac{\beta}{T_p^2}\right)$ vs. $\left(\frac{1}{T_p}\right)$, the slope can be used to calculate the activation energy.

2.3. Dynamic Mechanical Analysis (DMA)

Dynamic mechanical analysis (DMA) is a thermal analysis technique that measures the deformation of materials under periodic stress. The sinusoidal strain is measured depending on a variable applied sinusoidal stress. As a result, a phase difference occurs between the stress and strain waves that are used to determine storage modulus, loss modulus, and tan delta values (18). Storage modulus (E') is directly linked to the stiffness of a viscoelastic material. It is proportional to the stored energy. On the other hand, loss modulus (E'') represents the molecular motion of the material as the energy dissipation. The loss factor, also known as tan delta (tan δ) can be obtained by the ratio of loss and storage modulus values as shown below. As a result, it is a dimensionless parameter. It measures the damping behavior in a viscoelastic system(19).

$$\tan\delta = \frac{E''}{E'}$$

Materials do not have a single value as glass transition temperature is generally defined with a range of temperatures. The glass transition temperature (Tg) can be obtained from all these terms. Tg from the storage modulus is calculated from the onset of the storage modulus curve which is the lowest measured Tg. Storage modulus also generally informs about the mechanical strength of the material where begins to fail in terms of temperature. Tg values from loss modulus and tan δ are calculated from the maximum peak points. All these make DMA probably the most sensitive thermal technique for Tg determinations(20).

2.4. Fourier Transform Infrared Spectroscopy (FTIR)

The Fourier Transform Infra-Red Spectrometry (FTIR) is considered one of the most valuable analytical techniques to characterize and evaluate organic materials. In this study, FTIR spectroscopy was utilized to monitor the reaction of the polyurethane (21) and investigate the curing process as DSC and DMA.

FTIR has advantages over dispersive methods, including increased signal-to-noise ratio and the ability to obtain spectra of low energy, such as absorption bands with weak intensity. ATR was originally developed and commercialized for analyzing samples that are difficult to prepare or insoluble, such as rubbers and cured resins. The sample is placed in contact with an ATR crystal, one of the most used accessories for FTIR measurements, which absorbs near-infrared radiation and has a high refractive index. While some parts of the radiation penetrate the sample, and some parts are reflected. The depth of penetration of the beam depends on several parameters like the wavelength, angle of incidence, and refractive index of the crystal. Due to the requirement for close contact between the sample surface and the crystal, this method is not suitable for analyzing heterogeneous surfaces, such as many coatings. Additionally, weakly transparent and highly pigmented coatings are difficult to analyze using this technique. Since these kinds of disadvantages are not the subjects in our case, FTIR-ATR measurements for the samples are chosen as an alternative to being proof of DSC experimental and simulation results.

3. RESULTS AND DISCUSSION

3.1. DSC Results

Non-isothermal, isoconventional DSC method was used to investigate the curing process of a polyurethane system in the absence and the presence of dibutyltin dilaurate catalyst with different amounts. The typical DSC thermographs at different curing periods for different catalyst amounts were presented in Figure 2 from a to d as 0, 0.01, 0.1, and 0.5 phr (from C1 to C4), respectively. Due to the exothermic reaction of polyurethane, the curing peak exists in the exothermic area(22). While the black line represents the T_0 as just after the flash-off time (15 minutes later from the application), the red line shows the curing curve of the sample after 30 minutes at 80°C. The significant decrease in the exothermic curing peak is shown in the blue line that represents the DSC thermographs of significantly cured PUR samples. A decrease or total loss of the exothermic curing peaks means that the curing process is almost done at t_{final}. As shown in **Figure 2**, the endothermic peak areas decrease from a to d graphs and disappear for t_{final} curves. Especially for the maximum catalyst amounts it is more obvious. For example, for t_0 curves the dHc which is determined by the integrated area of the endothermic curing curve, decreases as 113, 102, 88, and 84 with increasing catalyst amount.

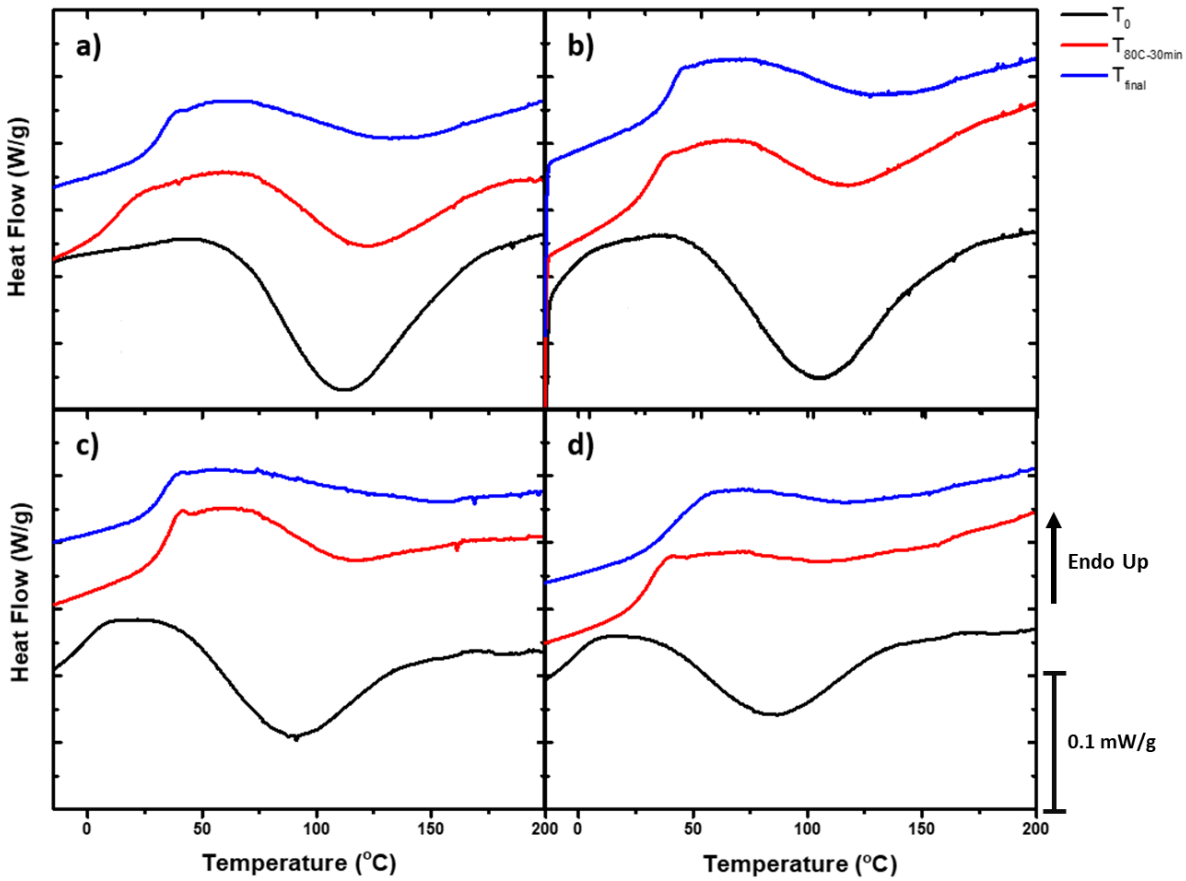

Figure 2. Typical endo up DSC curves for polyurethane coating with a) no catalyst, b) 0.01 phr, c) 0.1 phr, and d) 0.5 phr dibutyltin dilaurate catalyst amounts at different curing processes as T_0 (black), $T_{80C-30min}$ (red) and T_{final} (1 week after 30 minutes at 80°C annealing process and 15 minutes flash-off time) (blue).

Table 1. Kinetic parameters obtained regarding the 2nd order reaction kinetic according to the MRF for different catalyst amounts and curing times. The heating rate is 5°C/min.

Sample	Catalyst Amount	Curing Time	$T_{initial}$ (°C)	T_{peak} (°C)	ΔH_c (J/g)	Tg (°C)	Ea (kJ/mol)	a
C1	0	T_0	60	113	90.5	-	72.1	0.00
		$T_{80C-30min}$	73	122	36.9	15	84.0	0.57
		T_{final}	75	134	25.5	32	88.0	0.81
C2	0.01 phr	T_0	48	102	87.0	-	65.0	0.02
		$T_{80C-30min}$	70	117	30.4	28	81.4	0.66
		T_{final}	78	127	23.6	36	97.0	0.84
C3	0.1 phr	T_0	39	88	54.0	-1	70.8	0.40
		$T_{80C-30min}$	71	114	18.5	35	89.1	0.79
		T_{final}	-	-	-	33	81.0	0.88
C4	0.5 phr	T_0	38	84	39.6	2	73.0	0.53
		$T_{80C-30min}$	-	-	-	31	110.1	0.94
		T_{final}	-	-	-	44	155.2	0.96

As shown in Table 1, the important characteristic parameters such as initial curing temperature (T_i), peak curing temperature (T_p), and the enthalpy of curing reaction (ΔH_c) can be obtained by DSC thermographs. Ti and Tp values shift to the higher temperature values concerning conversion degree. ΔH_c was obtained by the simple kinetic model and Multilinear Regression fit (MRF). Similarly, the activation energies of the samples were directly obtained by MRF, too. Activation energies obtained from the whole samples increase for conversion degree (Figure 3a). Activation energy variation

concerning conversion may help to understand the type of process or reaction in different systems. Besides, a constant Ea value throughout the reaction process indicates that the single reaction type (addition reaction) dominates the curing in the polyurethane system(23). In epoxy systems, relatively stable Ea value may reduce at higher conversions which indicates the occurrence of autocatalytic effects (24). As in our case, increasing Ea with respect to conversion shows that the curing reaction is controlled mostly by diffusion rather than chemical reactions (3). The increasing trend of Ea with conversion is also correlated with similar studies that applied different modeling methods (15).

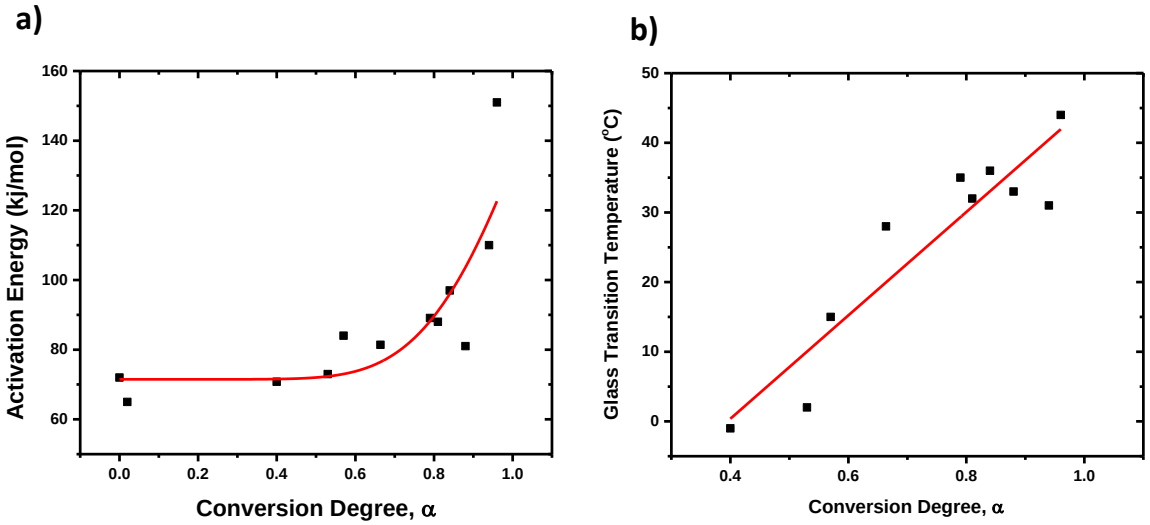

Figure 3. Variation of a) the activation energy and b) glass transition temperature with respect to the degree of conversion for all the studied samples.

The glass transition temperature of the samples is generally obtained from the second heat of DSC curves (25-27) to clear the history of the polymeric sample and smooth away the relaxation enthalpy. However, in our case, since a curing reaction exists in a DSC furnace only in one heating process, Tg was calculated from the first heating. It can be assumed that it is still reliable in terms of the accuracy Tg values in first and second heating do not change (unless heating and cooling temperatures exceed ±50K and change the structural composition of the polymeric chain). Commonly it is not possible to see the Tg for the samples at T_0, since the curing reaction does not start, and the polymeric structure is not formed. Increasing the curing time as $T_{80C\text{-}30min}$ and T_{final} samples, Tg becomes computable (Table 1). Tg increases with crosslinking density which also increases by the curing reaction of polyurethane system. Consequently, the direct relationship between Tg and conversion degree is observed as expected (Figure 3b). While the Tg of half-cured samples is 15°C, the cured samples have 44°C as the Tg value. The effect of the catalyst is also seen clearly that increasing the catalyst amount results in totally cured samples even in the samples with curing times 30 minutes at 80°C (C4). With the highest catalyst amount, half of the curing reaction was complete at T_0 that the curing exothermic peaks could not be observed for other sampling times. On the other hand, the samples without any catalyst did not completely cure even after 1 week. Similar phenomena were also observed in DMA analysis. The general trend and tan delta curves of the samples at Day 1 and 7 are shown in Figure 4a and b.

3.2 DMA Results

DMA analysis was performed on Day 1 and Day 7 for the samples without catalyst and with 0.01 and 0.5 phr catalyst. Because of the requirement of the free films for DMA analysis, it was not possible to analyze before Day 1 for each sample. Free films cannot be obtained for uncured samples. The significant change in Tg values between Day 1 and Day 7 obtained from storage modulus, loss modulus, and tan delta values are also shown in Figure 4a, clearly. Tan delta curves are also shown in Figure 4b. In the sample with the maximum catalyst used (C4), even on the first day, the samples have larger Tg values than the seventh day of the non-catalyzed sample (C1). These results which are comparable with DSC, show the significant effect of catalyst amount and the curing time on the total curing of the samples.

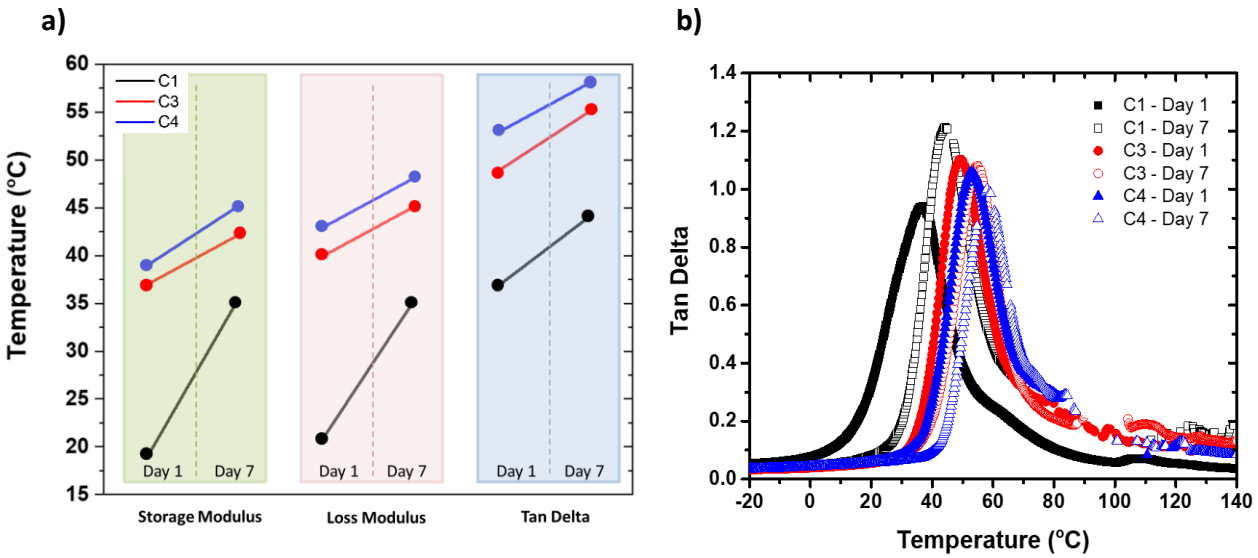

Figure 4. a) The difference in glass transition temperature (Tg) obtained from the onset of storage modulus, peak maximum of loss modulus, and tan delta values are given. b) Tan Delta values obtained by DMA for day 1 (filled) and 7 (holes) of the samples with different catalyst amounts 0, 0.01, and 0.5 phr as black, red, and blue, respectively. The shift in tan delta value between the first and the seventh days is more significant in the C1 sample.

3.3. FTIR Measurements

FTIR measurements were carried out for the samples for both unreacted reagents and the cured ones with different curing times as done in DSC measurements. FTIR has advantages over DMA measurements because all the samples can be measured without any limitations of the sample form.

Results showed the polyurethane structure with the typical carbonyl absorption band of the ester bond located at 1720 cm^{-1}, and another peak close to it at 1680 cm^{-1}, which is attributed to the urethane and urea carbonyl groups. The absorbance at around 3330 - 3380 cm^{-1} is consistent with the stretching of the NH bond and is characteristic of the urethane and urea groups. The other characteristic bands is 2940 cm^{-1} due to the alkane -CH stretching vibration (28). The main concerned peaks are the absorbance at 2270 cm^{-1} indicating unreacted isocyanate groups and 1680 cm^{-1} for the urethane peak. During the curing process, it is expected and monitored the absence of NCO peaks and the formation of urethane peaks.

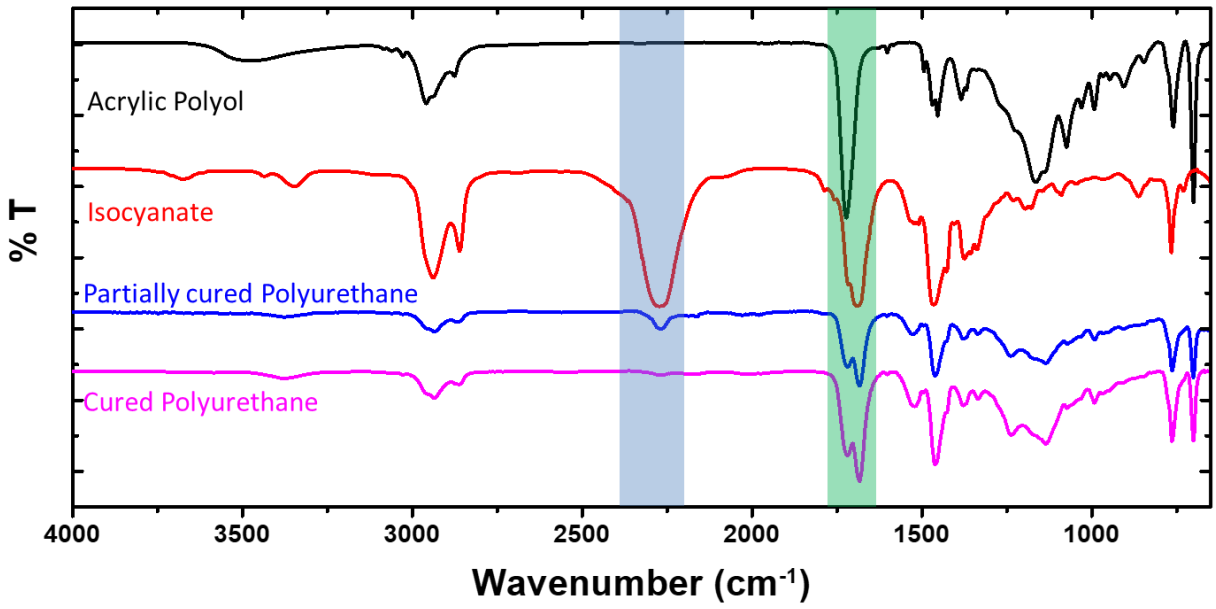

Figure 5. FTIR spectra of acrylic polyol, isocyanate, partially cured polyurethane, and fully cured polyurethane samples from up to down. While the blue region shows the NCO peak at 2270 cm^{-1}, green region shows C=O bond from both urethane and isocyanate molecule.

As mentioned before, the FTIR analysis was applied to prove both the experimental and simulation results of DSC measurements. For this purpose, samples were applied on glasses to obtain FTIR spectra. However, while the NCO peak at 2270 cm^{-1} was decreasing, we could not observe an increase in the 1680 cm^{-1} urethane peak (Figure S2) because of the matrix itself. In **Figure 5** the reference FTIR spectra are also shown that isocyanate also has an intense peak at 1680 cm^{-1} which comes from C=O bond of isocyanate chemical structure (Figure 6). As a result, it would not be possible to monitor the kinetic reaction of the polyurethanes because of the unobservable urethane peak in the same area. The curing reaction of polyurethane can be observed by monitoring the reduction of the NCO peak (Figure S2) by assuming all the NCO is converted to polyurethane and does not form urea by reacting with any water/humidity (29) in the environment, that may not be realistic.

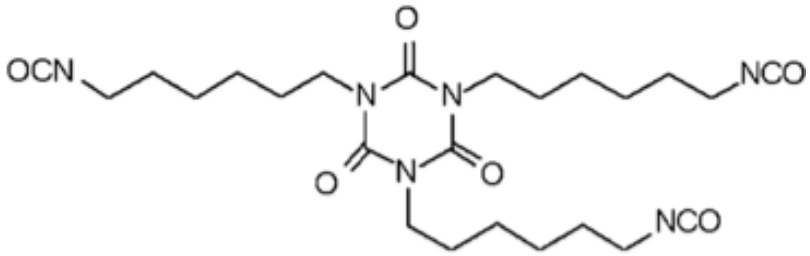

Figure 6. Chemical structure of HDI based isocyanate. C=O group in the cyclic structure results signal at 1680 cm^{-1} in FTIR spectra.

These limitations show that FTIR may not be a suitable measurement, as DMA. That is the reason DSC techniques was discussed for the further study.

3.4 Model-Free Kinetic Calculations

In this study, Multiple Regression Fit (MRF) was used essentially in terms of easy handling of kinetic parameters and fast results due to the sufficiency of single-rate heating curves. However, Ozawa and Kissinger's methods were also distinguished to investigate the possible differences between the results obtained from single-rate and multi-rate heating curves. For this purpose, curing analysis was applied to the samples with different heating rates as 2.5, 5, 10, and 20 K/min. Two different samples (C1-C2) were studied with two methods to compare the kinetic parameters. As shown in Figure S3 the kinetic parameters like T_i and T_p shift to the higher temperatures with the increase in the heating rate. Similarly, the signal intensity of the whole curve increases, and Tg and curing peaks become more visible with higher heating rates. The reason for this phenomenon can be explained by the fact that the curing reaction is not only a thermodynamic process but also a dynamic process. In the case of using lower heating rates, the reactants find sufficient time to react with each other. So, relatively lower curing initial and peak temperature values are obtained at lower heating rates(30). Since the thermal effect per unit time increases, the enthalpy of the system also increases(31). The data obtained from Figure S3 were used to obtain Ea values from Ozawa and Kissinger equations.

The plots that were mentioned before for Ozawa and Kissinger methods are shown in Figure 7, and the obtained kinetic parameters are given in Table S1. The straight line of the slope was obtained for both models to calculate the kinetic parameters. Calculated activated energies were very close to Ozawa and Kissinger's methods. The activation energies for the C1 sample are 24.1 kJ/mol and 23.3 kJ/mol obtained from the Ozawa and Kissinger methods, respectively with a 0.9997 correlation factor. For the other sample, activation energies were 19.5 and 19.2 kJ/mol for the Ozawa and Kissinger methods, respectively with relatively the same correlation coefficients. The results also showed that the Ea of the curing system decreases after the addition of catalyst which proves that the reaction system is more rapid with the catalyst. (31)

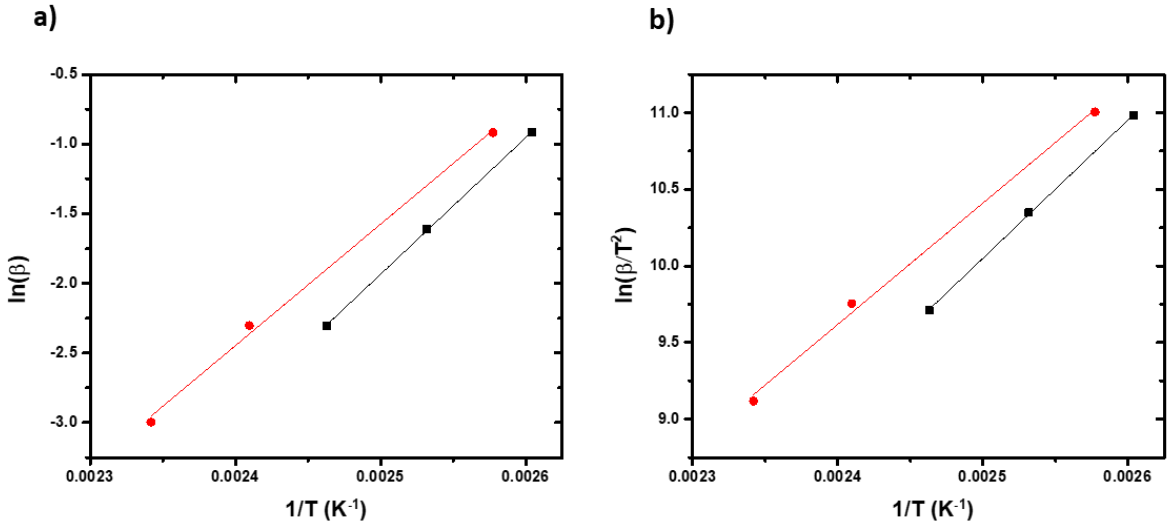

Figure 7. a) Ozawa and b) Kissinger plot of C1 (black) and C2 (red) samples with curing time 30 minutes at 80°C. The slope of the graphs is linear, and the activation energies obtained from both methods gave similar values with high correlation coefficients.

3.5. Isothermal Prediction Calculations

As mentioned before, MRF results were applied for all samples because of the easy and fast availability of the curing results. The isothermal prediction curves in terms of % conversion with respect to reaction time or isothermal temperature were also obtained from MRF simulations. As with all other similar simulation software, the results do not give certain values but comparable approximations. In Figure 8 the isothermal conversion predictive curves for the samples without a catalyst at different sampling times, t_0 and t_{final} are shown. The effect of curing time in terms of curing reaction kinetic is seen in this simulation.

As shown in Figure 8a, 5 minutes under 100 °C isothermal reaction temperature is enough for a 40% conversion degree for the t0 sampling. On the other hand, approximately 125 °C isothermal reaction temperature or 20 minutes at the same temperature is necessary for the same conversion degree when a significantly (81% of cured, Table 1) cured sample (tfinal sampling). Similarly, to achieve 90% conversion for t0 sampling, 100 minutes at almost 65 °C is required. However, for the same reaction time, the reaction temperature should be increased up to 110 °C to achieve the same conversion degree in the 81% cured samples. At first sight, the expectation can be vice versa that one expects that the almost cured sample should require minimum reaction time or lower isothermal reaction temperatures. However as mentioned before, in our system diffusion-controlled reaction mechanism is more dominant than the chemical reaction (3). In other words, it decreases the ion mobility, increases the crosslinking density of the matrix, and reduces the reaction rate. Figure 8b explains this phenomenon from different aspects that the relatively low reaction rate in 81% cured sample can be understood clearly. While for the cured sample 70% conversion can only be achieved in 60 minutes at 100 °C, the same conversion can be achieved in 15 minutes at the same reaction temperature.

The effect of catalyst amount on the curing kinetic is shown in Figure 9. For all samples, t0 sampling was considered to ignore the effect of diffusion-reaction related to the reaction time. As shown in Figure 9a, increasing the catalyst amount % conversion increases. As an example, the % conversion of the samples with 0, 0.01, and 0.5 phr catalyst amounts increases as 10%, 20%, and 40%, respectively for 5 minutes of reaction time at 75 °C isothermal reaction temperature. Similarly, at 100 °C, for an 80% conversion degree, 5 minutes is enough for the sample with the maximum catalyst amount. For 0.01 phr and no catalyst samples, the required reaction times for the same circumstances are 20 minutes and 30 minutes, respectively. Figure 9b, % conversion with respect to reaction time under isothermal reaction temperatures are shown for the same samples. The catalyst effect is deducible when reaction times for 90% conversion degrees at 100 °C isothermal reaction temperatures are considered. While 10 minutes reaction time is enough with the maximum amount of catalyst existing, required reaction times increase to 30 minutes and 60 minutes for the 0.01 phr and no catalyst samples, respectively. Figure S4 can give a similar idea about the curing kinetics by the graphs of isothermal reaction temperatures vs reaction time curves in different conversion degrees for the samples with different catalyst amounts.

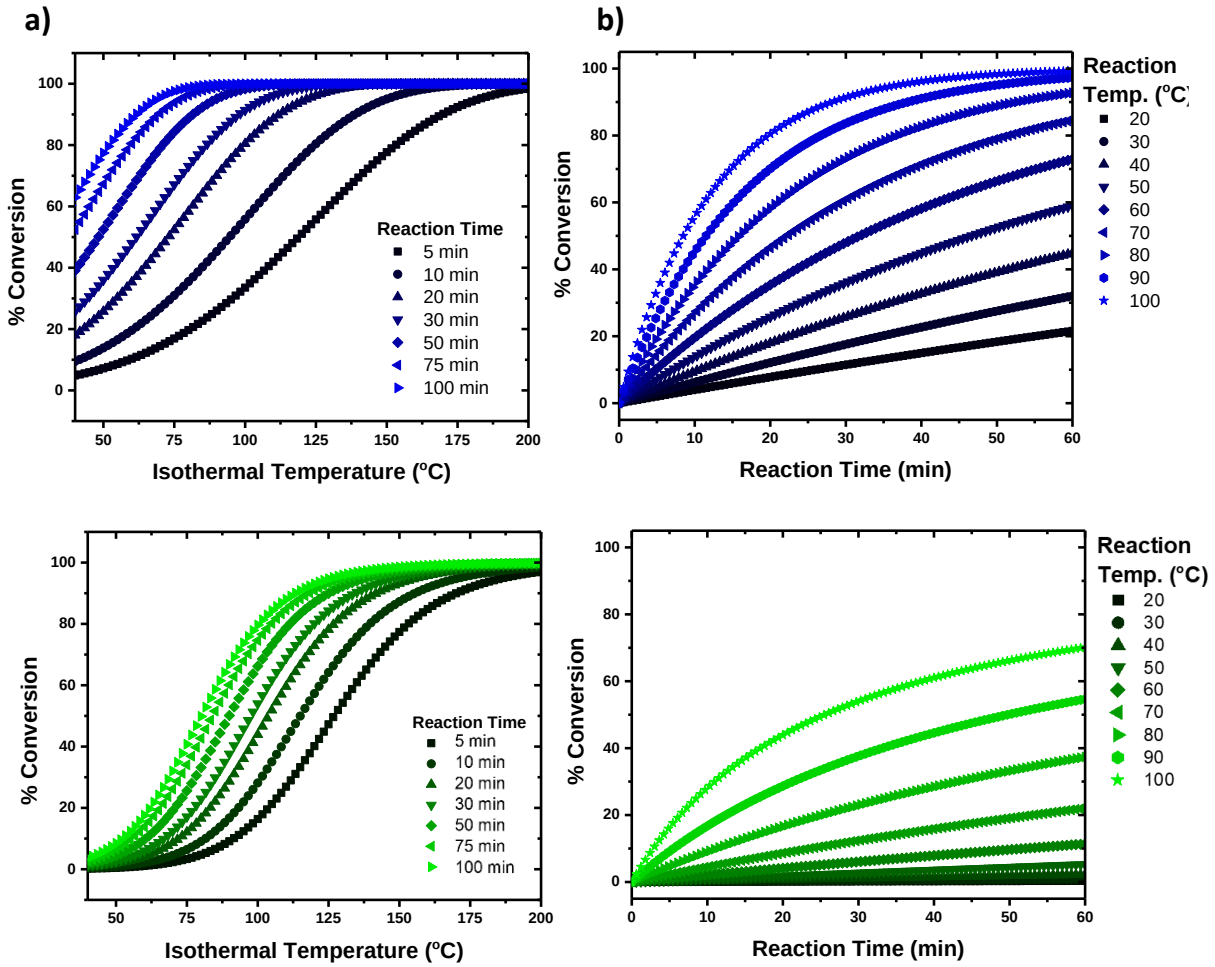

Figure 8. Isothermal conversion predictive curves for the sample without catalyst (C1) at t_0 sampling (blue) and t_{final} sampling (green) to show the effect of curing time. a) % Conversion vs. isothermal temperature for different reaction times and b) % conversion vs reaction time for different isothermal reaction temperatures were shown.

The basic idea obtained from all the isothermal prediction curves gives information about the reaction rate of the samples with dependence on the curing time and the catalyst amount. Figure 10 summarizes both explanations in one graph in which the rate constant of two samples (C1, without any catalyst, and C4 with the maximum amount of catalyst) are given with respect to reaction temperature at different curing times. The existence of the catalyst increases the rate of the reaction which is more significant after 75 °C. However, the rate constant variation at room temperature (25 °C) also obey the trend that the catalyst amount increases the rate of reaction significantly and the degree of curing effects it, too. The curing temperature is directly linked to the diffusion reaction, in other words, the ion mobility and the crosslink density of the system result decrease in the rate constant, as expected.

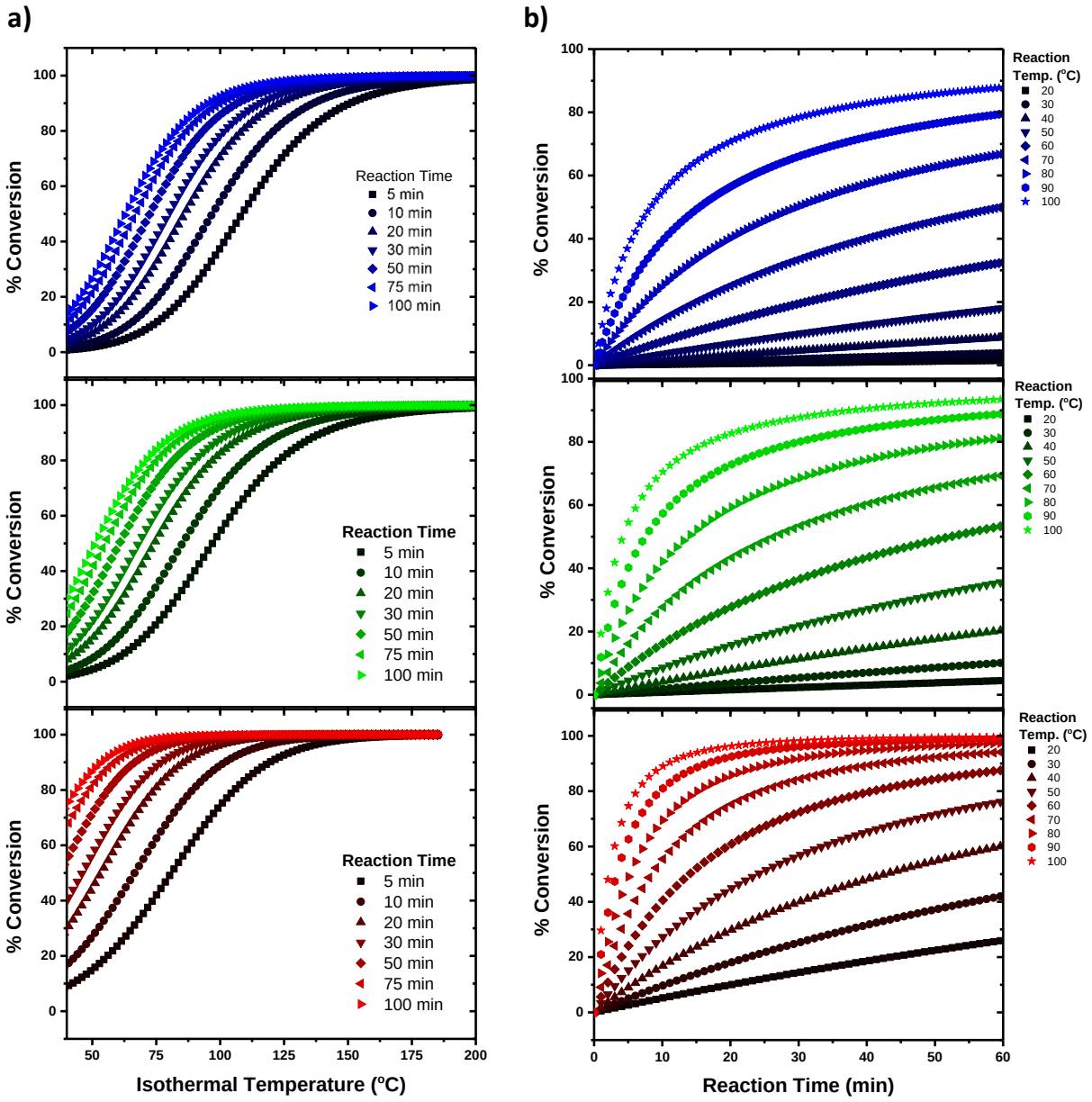

Figure 9. Isothermal conversion predictive curves for C1 (Blue), C2 (green), and C4 (red) samples to understand the effect of catalyst amount. Conversion vs. a) isothermal temperature and b) time curves are shown for different reaction times and reaction temperatures, respectively.

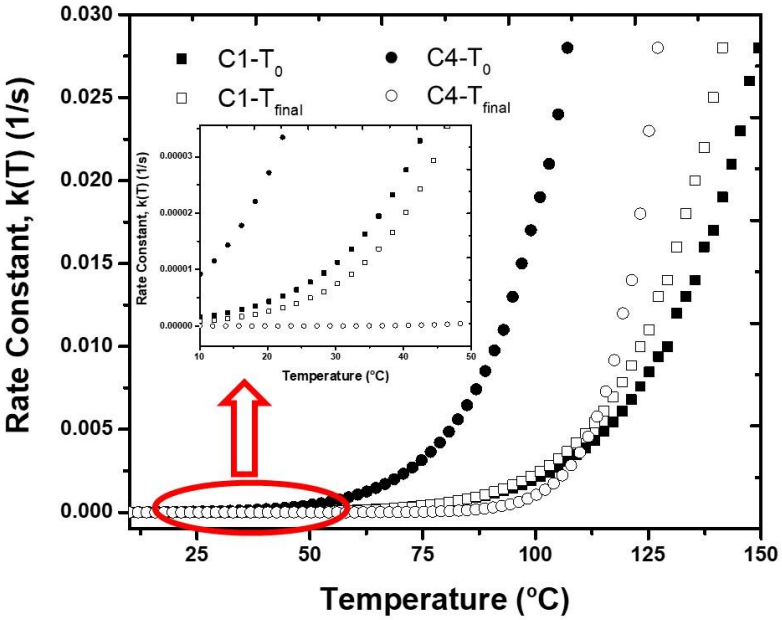

Figure 10. The rate constant of the sample without catalyst (C1) and the maximum amount of catalyst (C4) for t_0 and T_{final} curing times. For each case, the final samples have lower reaction rates for all reaction temperatures.

All these prediction curves simulate valuable results to estimate the curing kinetics of any system under different reaction conditions like catalyst amounts, reaction time temperatures, etc. Especially for industrial-scale production cases, kinetic estimations are more critical.

4. CONCLUSION

In this study, the two major aims of kinetic analysis, to clarify the reaction mechanism with kinetic parameters and to predict the kinetic characteristic of the materials under different reaction parameters were aimed and achieved by both DSC and DMA analysis. Both thermal analysis results confirm each other however, the restrictions of the sample preparation in DMA limit understanding of the kinetic mechanism in lower reaction times. That is the reason, DSC analysis was preferred in terms of its ability to obtain lots of kinetic information. The effect of the curing time and the amount of DBTL catalyst on polyurethane reaction kinetics were investigated by single and multi-heating methods to understand the kinetic characteristic of the reaction. The simple kinetic model and Multilinear Regression fit (MRF) were used to calculate the kinetic parameters and simulate the isothermal prediction curves.

The results showed that the curing time and the catalyst amount affect the kinetic process of polyurethane reactions regarding the specific reactants and the catalyst. Tg values of the samplings of the same curing times increase with respect to catalyst amounts. Undeterminable Tg values for t0 sampling with no and lower catalyst amounts became detectable with the increase of catalyst. Similarly, the maximum Tg value was obtained by the maximum catalyst amount as 44 °C. The conversion degrees confirm the Tg values in which there is a direct relation between each other. The activation energy of any case in our system increases with the increase in conversion degree. Diffusion-controlled reaction mechanism results in a decrease in the reaction rate due to the increased crosslinked matrix. A decrease in the number of reactants and less reactive reagents because of the high-dense medium makes it difficult to continue the reaction, so the activation energy increases.

Isothermal prediction curves were studied to simulate the curing behavior of the polyurethane matrix under different isothermal temperatures and reaction times. Curves showed that final samples have lower conversion than the initial samples for the same reaction conditions, due to the diffusion controlled mechanism. In the case of different catalyst amounts, for the initial sampling time, the higher catalyst amount sample has significantly higher conversion. Since there is no high-dense medium because of the consideration of the initial samplings, the diffusion-controlled mechanism does not affect the reaction kinetics.

The kinetic calculations and the isothermal prediction curve are critical in terms of real-life applications, especially in the coating industry. The optimization of the curing conditions for a specific system may require lots of experimental procedures unless kinetic approximations are applied. On the other hand, the information obtained from these calculations can be used to provide the required conditions to obtain fully cured samples even after the first curing procedures. Current study also prove simple and effective way to understand the optimization of organic coating indication different systems with different catalyst.

5. CONFLICT OF INTEREST

There is no conflict of interest in this study.

7. REFERENCES

1. Groenewolt M. Polyurethane coatings: a perfect product class for the design of modern automotive clearcoats. Polymer International. 2019;68(5):843-7. Available from: <URL>.

2. Li K, Gan C, Zhang W, Li C, Li G. Validity of isothermal kinetic prediction by advanced isoconversional method. Chemical Physics. 2023;567:111801. Available from: <URL>.

3. Yi C, Rostron P, Vahdati N, Gunister E, Alfantazi A. Curing kinetics and mechanical properties of epoxy based coatings: The influence of added solvent. Progress in Organic Coatings. 2018;124:165-74. Available from: <URL>.

4. Liu S, Li X, Ge M, Du X, Zou M. Curing Kinetics of Methylene Diphenyl Diisocyanate–Based Polyurethane Elastomers. Polymers. 2022;14(17):3525. Available from: <URL>.

5. Manu SK, Sekkar V, Scariah KJ, Varghese TL, Mathew S. Kinetics of glycidyl azide polymer-based urethane network formation. Journal of Applied Polymer Science. 2008;110(2):908-14. Available from: <URL>.

6. Shundo A, Yamamoto S, Tanaka K. Network Formation and Physical Properties of Epoxy Resins for Future Practical Applications. JACS Au. 2022;2(7):1522-42. Available from: <URL>.

7. Balakrishnan R, Nallaperumal AM, Manu SKP, Varghese LA, Sekkar V. DSC assisted kinetic analysis on the urethane network formation between castor oil based ester polyol and poly(methylene di phenyl isocyanate) (pMDI). International Journal of Polymer Analysis and Characterization. 2022;27(2):132-46. Available from: <URL>.

8. Balakrishnan R, Soumyamol PB, Vijayalakshmi KP, Alen Varghese L, Rajeev R, Manu SK, et al. Kinetic analysis of urethane formation between castor oil-based ester polyol and 4,4'-diphenyl methane diisocyanate. Indian Chemical Engineer. 2021;63(5):491-500. Available from: <URL>.

9. Hui M, Yu-Cun L, Tao C, Tuo-Ping H, Jia-Hu G, Yan-Wu Y, et al. Kinetic studies on the cure reaction of hydroxyl-terminated polybutadiene based polyurethane with variable catalysts by differential scanning calorimetry. e-Polymers. 2017;17(1):89-94. Available from: <URL>.

10. Schuster F, Ngako Ngamgoue F, Goetz T, Hirth T, Weber A, Bach M. Investigations of a catalyst system regarding the foamability of polyurethanes for reactive inkjet printing. Journal of Materials Chemistry C. 2017;5(27):6738-44. Available from: <URL>.

11. Kaushik A, Singh P. Kinetic Study of Polyurethane Reaction between Castor Oil/TMP Polyol and Diphenyl Methane Diisocyanate in Bulk. International Journal of Polymeric Materials and Polymeric Biomaterials. 2006;55(8):549-61. Available from: <URL>.

12. Vyazovkin S, Burnham AK, Criado JM, Pérez-Maqueda LA, Popescu C, Sbirrazzuoli N. ICTAC Kinetics Committee recommendations for performing kinetic computations on thermal analysis data. Thermochimica Acta. 2011;520(1):1-19. Available from: <URL>.

13. Keskin S, Özkar S. Kinetics of polyurethane formation between glycidyl azide polymer and a triisocyanate. Journal of Applied Polymer Science. 2001;81(4):918-23. Available from: <URL>.

14. Kilivnik YN, Lipatova TE. The kinetics of formation of a crosslinked polyurethane in the presence of magnesium ions. Polymer Science USSR. 1976;18(12):3017-23. Available from: <URL>.

15. Stanko M, Stommel M. Kinetic Prediction of Fast Curing Polyurethane Resins by Model-Free Isoconversional Methods. Polymers. 2018;10(7):698. Available from: <URL>.

16. Cui H-W, Suganuma K, Uchida H. Using the Ozawa method to study the thermally initiated curing kinetics of vinyl ester resin. RSC Advances. 2015;5(4):2677-83. Available from: <URL>.

17. Vyazovkin S. Kissinger Method in Kinetics of Materials: Things to Beware and Be Aware of. Molecules. 2020;25(12). Available from: <URL>.

18. Shamsi R, Mir Mohamad Sadeghi G, Asghari GH. Dynamic mechanical analysis of polyurethanes and carbon nanotube based composites obtained from PET waste. Polymer Composites. 2018;39(S2):E754-E64. Available from: <URL>.

19. Shen Y, Tan J, Fernandes L, Qu Z, Li Y. Dynamic Mechanical Analysis on Delaminated Flax Fiber Reinforced Composites. Materials. 2019;12(16):2559. Available from: <URL>.

20. Bertotto MM, Gastón A, Rodríguez Batiller MJ, Calello P. Comparison of mathematical models to predict glass transition temperature of rice (cultivar IRGA 424) measured by dynamic mechanical analysis. Food Sci Nutr. 2018;6(8):2199-209. Available from: <URL>.

21. Dias RCM, Góes AM, Serakides R, Ayres E, Oréfice RL. Porous biodegradable polyurethane nanocomposites: preparation, characterization, and biocompatibility tests. Materials Research. 2010;13. Available from: <URL>.

22. Zhang B, Wang B, Zhong Y, Wang S, Li X, Wang L. Experimental Study on Reducing the Heat of Curing Reaction of Polyurethane Polymer Grouting

Material. Advances in Polymer Technology. 2021;2021:9954498. Available from: <URL>.

23. Remya Balakrishnan LAV, K Manu. Cure kinetics and thermodynamics of polyurethane network formation based on castor oil based polyester polyol and 4,4'-diphenyl methane diisocyanate. Indian Journal of Chemical Technology. 2021;28(3):7. Available from: <URL>.

24. Tziamtzi CK, Chrissafis K. Optimization of a commercial epoxy curing cycle via DSC data kinetics modelling and TTT plot construction. Polymer. 2021;230:124091. Available from: <URL>.

25. Hong JU, Lee TH, Oh D, Paik H-j, Noh SM. Scratch-healable automotive clearcoats based on disulfide polyacrylate urethane networks. Progress in Organic Coatings. 2021;161:106472. Available from: <URL>.

26. Sáenz-Pérez M, Lizundia E, Laza JM, García-Barrasa J, Vilas JL, León LM. Methylene diphenyl diisocyanate (MDI) and toluene diisocyanate (TDI) based polyurethanes: thermal, shape-memory and mechanical behavior. RSC Advances. 2016;6(73):69094-102. Available from: <URL>.

27. Cuevas JM, Cobos R, Germán L, Sierra B, Laza JM, Vilas-Vilela JL. Enhanced mar/scratch resistance in automotive clear coatings by modifying crosslinked polyurethane network with branched flexible oligomers. Progress in Organic Coatings. 2022;163:106668. Available from: <URL>.

28. Lee H-T, Lin L-H. Waterborne Polyurethane/Clay Nanocomposites: Novel Effects of the Clay and Its Interlayer Ions on the Morphology and Physical and Electrical Properties. Macromolecules. 2006;39(18):6133-41. Available from: <URL>.

29. Shi Y, Zhan X, Luo Z, Zhang Q, Chen F. Quantitative IR characterization of urea groups in waterborne polyurethanes. Journal of Polymer Science Part A: Polymer Chemistry. 2008;46(7):2433-44. Available from: <URL>.

30. Yin H, Sun DW, Li B, Liu YT, Ran QP, Liu JP. DSC and curing kinetics study of epoxy grouting diluted with furfural -acetone slurry. IOP Conference Series: Materials Science and Engineering. 2016;137(1):012001. Available from: <URL>.

31. Ma H, Zhang X, Ju F, Tsai S-B. A Study on Curing Kinetics of Nano-Phase Modified Epoxy Resin. Scientific Reports. 2018;8(1):3045. Available from: <URL>.